

# Geometric phases distinguish entangled states in wormhole quantum mechanics

Flavio S. Nogueira,<sup>1</sup> Souvik Banerjee,<sup>2,3</sup> Moritz Dorband,<sup>2,3</sup>  
René Meyer,<sup>2,3</sup> Jeroen van den Brink,<sup>1,3,4</sup> and Johanna Erdmenger<sup>2,3</sup>

<sup>1</sup>*Institute for Theoretical Solid State Physics, IFW Dresden, 01069 Dresden, Germany*

<sup>2</sup>*Institute for Theoretical Physics and Astrophysics,  
Julius-Maximilians-Universität Würzburg, 97074 Würzburg, Germany*

<sup>3</sup>*Würzburg-Dresden Cluster of Excellence ct.qmat*

<sup>4</sup>*Institute for Theoretical Physics, TU Dresden, 01069 Dresden, Germany*

We establish a relation between entanglement in simple quantum mechanical qubit systems and in wormhole physics as considered in the context of the AdS/CFT correspondence. We show that in both cases, states with the same entanglement structure, indistinguishable by any local measurement, nevertheless are characterized by a different Berry phase. This feature is experimentally accessible in coupled qubit systems where states with different Berry phase are related by unitary transformations. In the wormhole case, these transformations are identified with a time evolution of one of the two throats.

In recent years, significant progress has been achieved in establishing new relations between geometry and gravity on the one hand, and quantum entanglement on the other. An important example is provided by the Ryu-Takayanagi formula [1] in the context of the AdS/CFT correspondence [2] that relates the entanglement entropy of a conformal field theory to the area of a minimal surface in Anti-de Sitter (AdS) space. Moreover, in the ER=EPR conjecture [3] it is argued that the entanglement in a thermofield double (TFD) state is realized by a geodesic in a non-traversable wormhole in AdS space.

Within a simpler setting, examples for wormholes are realized in electrodynamics and quantum mechanics. An early example is the semiclassical Wheeler wormhole, that gives rise to so called “geons” [4], as discussed in [5]. This is a particular solution of Maxwell theory involving a magnetic flux. Its causal structure is similar to a non-traversable wormhole in gravity. An important feature of this solution is that the magnetic field involved cannot be globally written in terms of a vector potential. Mathematically, this amounts to a non-exact symplectic form, yielding a quantized flux, similarly to a magnetic monopole [6].

Recently, H. Verlinde [7] studied quantum-mechanical examples of wormholes by analyzing their partition functions. A particularly simple realization is provided by coupled harmonic oscillators. For systems with a non-exact symplectic form, the thermal partition function becomes a functional integral over a two-dimensional surface, and corresponds to the Renyi entropy of a thermal mixed state.

In this letter we note further surprising similarities between a simple coupled two-qubit system in quantum mechanics and spacetime wormholes in gravity. For the gravity analysis, we focus on the entanglement structure of an eternal black hole in AdS space. This black hole is assumed to be dual to a maximally entangled state of two decoupled CFTs living on the left ( $L$ ) and right ( $R$ ) boundaries in the TFD state [8] (Fig. 1). As shown

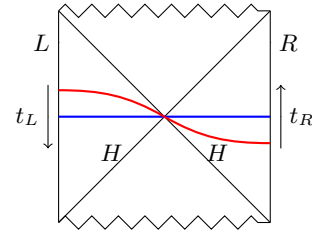


FIG. 1. Kruskal diagram of the eternal Schwarzschild black hole in AdS with time in the vertical and spatial coordinates in the horizontal direction. Vertical lines denote the left ( $L$ ) and right ( $R$ ) asymptotic boundaries where the CFTs are defined. The jagged lines are the singularities and diagonal lines represent the black hole horizon ( $H$ ). The blue line corresponds to the wormhole dual to the original TFD state while the red one corresponds to a time-shifted wormhole. The arrows indicate the directions of time in the boundary theories.

in [9, 10], there exists a class of time-shifted wormholes dual to states related to the original TFD state by a phase  $\alpha_n$ . These arise from unequal time evolution of the boundaries. From the perspective of the bulk AdS geometry, these phase-shifted states correspond to the same wormhole geometry, but with different asymptotic identifications of the boundary times. Such phase-shifted states have the same entanglement properties as the TFD state. However, their Berry phases are different. This is a consequence of the fact that a gravitational system in the presence of black holes does not have a globally defined time.

Here we show that by distinguishing between states with the same entanglement, the Berry phases with respect to this phase-shifted parameter provide a precise analogue to the entanglement structure of coupled quantum spins in a magnetic field. By determining the Berry phase for entangled states of two coupled spins with respect to the magnetic field, we indeed directly find that different states related by unitary transformations, and thus sharing the same entanglement structure, have nevertheless different Berry phases. Furthermore, as we will show following [7], in both our quantum spin system and

in gravity, this behavior traces back to the presence of a non-exact symplectic form. Physically, the quantum spin model with geometric and entanglement structure equivalent to the wormhole is realized by a hydrogen atom with hyperfine coupling between proton and electron spin. On a next level of abstraction, it corresponds to a specific pair of entangled qubits. Consequently, the equivalent relation between entanglement structure and Berry phases in the gravitational wormhole context can be probed experimentally by quantum-state tomography [11] on this specific qubit pair. We will explicitly return to this point at the end of our discussion.

*Unitary transformations and Berry phase: coupled quantum spins* — To set the stage, we first consider the entanglement structure of a hydrogen atom with hyperfine coupling  $J$  between proton and electron spins in magnetic field. In first approximation, the Zeeman coupling to the proton spin can be neglected and the system is described by the Hamiltonian,

$$H = J\mathbf{S}_1 \cdot \mathbf{S}_2 - 2\mu_B B S_{1z}, \quad (1)$$

where the second term is the electronic Zeeman interaction. The ground state with energy  $E_0 = -J/4 - \sqrt{J^2/4 + (\mu_B B)^2}$  is given by

$$|\psi_0\rangle = -\sin\left(\frac{\alpha}{2}\right)|1, 0\rangle + \cos\left(\frac{\alpha}{2}\right)|0, 0\rangle, \quad (2)$$

in terms of the singlet and triplet states  $|s, m\rangle$  and  $\tan\alpha = 2\mu_B B/J$ . For our analysis we generalise the Hamiltonian (1) to an arbitrary coupling term  $\propto \mathbf{B} \cdot \mathbf{S}_1$ . Then we apply unitary transformations on the spins designed such that the interaction term reduces back to the form in (1). While this restricts the transformation on the first spin to

$$U_1(\varphi, \theta) = e^{-i\varphi S_{1z}} e^{-i\theta S_{1y}} e^{i\varphi S_{1z}}, \quad (3)$$

we are free to choose what transformation to use on the second spin. We employ the transformation  $U_2(\varphi, \theta) = U_1(\lambda\varphi, \lambda\theta)$  with a parameter  $\lambda \in [0, 1]$  interpolating between  $U_2 = \mathbb{1}$  for  $\lambda = 0$  and  $U_2 = U_1$  for  $\lambda = 1$ .

The entanglement entropy between the spins is not affected by the application of a unitary transformation  $U = U_1 \otimes U_2$ , in which  $U_1$  and  $U_2$  only act on their respective subsystem. As derived in the appendix, the entanglement entropy for the  $i$ -th spin is given by

$$S_{\text{EE}}^i(\text{tr}_j(|\psi_0\rangle\langle\psi_0|)) = S_{\text{EE}}^i(\text{tr}_j(U|\psi_0\rangle\langle\psi_0|U^\dagger)), \quad (4)$$

where  $i, j \in \{1, 2\}$  and  $i \neq j$ . Despite the entanglement entropy being unaffected by the application of  $U = U_1 \otimes U_2$ , we find different Berry phases for every  $\lambda$ , as we will now discuss in detail.

*Berry phase probing the hyperfine structure of entanglement* — To define the Berry connection for the setup discussed above, we make use of the Maurer-Cartan form

[12]. This is the natural connection on a group manifold  $\mathcal{M}$  and is defined for any group element  $\sigma \in \mathcal{M}$  as  $A_{\text{MC}} = \sigma^{-1}d\sigma$ . The group element we choose in our example is the unitary transformation  $U$ . The Berry connection is then given by the expectation value of the Maurer-Cartan form for the ground state (2),

$$\begin{aligned} A_{\text{B}}(\lambda) &= i\langle\psi_0|A_{\text{MC}}|\psi_0\rangle = i\langle\psi_0|(U^\dagger dU)|\psi_0\rangle \\ &= \frac{\sin\alpha}{2}\{(1 - \cos\theta) - \lambda[1 - \cos(\lambda\theta)]\}d\varphi. \end{aligned} \quad (5)$$

From the connection we define the associated symplectic form, known as Kirillov-Kostant form  $\omega_{\text{KK}} = dA_{\text{MC}}$  [12]. Calculating the expectation value for the ground-state yields the Berry curvature

$$\begin{aligned} F_{\text{B}}(\lambda) &= i\langle\psi_0|\omega_{\text{KK}}|\psi_0\rangle \\ &= \frac{\sin\alpha}{2}(\sin\theta - \lambda^2\sin(\lambda\theta))d\theta \wedge d\varphi. \end{aligned} \quad (6)$$

Both (5) and (6) are non-trivial as long as  $\lambda \neq 1$ . While acting with the same transformation on both subsystems does not yield a Berry phase, a non-trivial result is found if these transformations are different. The key observation here is that the Berry phase of these states depends on  $\lambda$ , whereas (4) shows that the entanglement entropy of each subsystem is insensitive to it. We expect that this feature can be converted into an experimental tool which may be used to differentiate between two such states that have indistinguishable entanglement properties.

In two dimensions, the symplectic form is proportional to the volume form. The space in our case being just compact  $S^2$ , the symplectic form, and equivalently the Berry curvature cannot be globally exact. This non-exactness of the symplectic form can be understood from the following group theoretic argument, which will also explain the relative sign appearing in the final expression of (6).

*Berry phase and non-exact symplectic structure* — To pinpoint the presence of a non-exact symplectic form in the entangled two-spin system, we consider a group theoretic approach to obtain the Berry connection corresponding to the Hamiltonian (1) and the unitary transformation  $U$ . A single spin  $\mathbf{S}$  can be represented in  $\mathbf{CP}^1$  variables  $z_i$ ,

$$\mathbf{S} = \frac{1}{2}z_i^* \boldsymbol{\sigma}^{ij} z_j. \quad (7)$$

This is essentially a Schwinger boson representation which upon quantization,  $z_i^{(*)}$  represent annihilation (creation) operators. For the two-spin model discussed we may introduce  $\mathbf{CP}^1$  variables for each spin, which in absence of an external field leads to a tensor product structure  $\mathbf{CP}^1 \times \mathbf{CP}^1$  that can also be realized as a diagonal embedding into  $\mathbf{CP}^3$ . Including the Zeeman term as in (1) breaks the tensor product structure. By this analysis we can also understand the Berry phase arising for different unitaries.

The  $\mathbf{CP}^3$  structure provides a natural way to define a connection as follows.  $\mathbf{CP}^3$  can be constructed as a coset space  $\mathbf{CP}^3 = \frac{\text{SU}(4)}{\text{U}(3)}$ . The  $\text{U}(1)$  factor in  $\text{U}(3)$  can be used to define a  $\text{U}(1)$  bundle. Its connection is the Maurer-Cartan form. The symplectic form follows as the exterior derivative of the connection. Since in the presence of the magnetic field, the state (2) does not lie inside the natural  $\mathbf{CP}^1 \times \mathbf{CP}^1 \subset \mathbf{CP}^3$  submanifold, we are forced to consider the Berry connection inside the full  $\text{U}(1)$  bundle given by  $\mathbf{CP}^3$ . In particular, the state evolution given by the path  $U(\lambda) = U_1 \otimes U_2(\lambda)$  gives rise to a Berry connection (6) on the full  $\mathbf{CP}^3$  bundle.

For a general group element  $g \in \text{SU}(4)$  as appearing in the coset construction of  $\mathbf{CP}^3$ , the connection in the  $\text{U}(1)$  fibre is defined as

$$A = i \text{tr}(t_{\text{U}(1)} A_{\text{MC}}(g)). \quad (8)$$

Here,  $t_{\text{U}(1)}$  corresponds to the generator of  $\text{SU}(4)$  yielding the  $\text{U}(1)$  factor of  $\text{U}(3)$  given by

$$t_{\text{U}(1)} = \frac{1}{\sqrt{24}} \text{diag}(1, 1, 1, -3). \quad (9)$$

To obtain the connection for the Hamiltonian (1), we pick the transformation  $U$  as group element of  $\text{SU}(4)$ . Note that this group element only belongs to the factorised subgroup  $\text{SU}(2) \times \text{SU}(2)$ . However,  $\text{SU}(4) \supset \text{SU}(2) \times \text{SU}(2) \times \text{U}(1)$  where the  $\text{U}(1)$  factor rotates in the first  $\text{SU}(2)$  subspace with a positive phase, and in the second  $\text{SU}(2)$  subspace with the opposite phase [13]. To account for this relative sign in our transformation  $U(\lambda)$ , we have to replace  $\sigma_i \rightarrow -\sigma_i$  in the transformation acting only on the second spin,  $U_2 \rightarrow \tilde{U}_2 = U_2^T$ . Inserting (9) into (8) and considering  $g = U_1 \otimes \tilde{U}_2$ , we find the same connection as given in (5). For more details on this calculation we refer the reader to the appendix.

Following the argument of [7], we identify the non-exact Berry curvature (6) as a signature for a wormhole structure. As discussed above, this structure arises from non-diagonally embedded submanifolds of  $\mathbf{CP}^3$ . It is not manifest for the diagonal embedding  $\mathbf{CP}^1 \times \mathbf{CP}^1$ .

Next, we show that the non-exact symplectic structure with corresponding Berry phase, which becomes manifest in the  $\mathbf{CP}^3$  embedding, is also present in actual spacetime wormholes. This confirms that wormhole-like features are present both in gravity and in quantum mechanics. However, in quantum mechanics such a structure is not evident when we only focus on the diagonal subgroup of the full symmetry group, which already assumes a factorized structure of the Hilbert space. As evident from the discussion above, the correlations present in the emergent wormhole show up in the Berry connection whenever different unitary transformations act upon the two spins.

*Unitary transformations and Berry phase: gravitational wormholes* — The group-theory and entanglement structures obtained for the two-spin quantum mechanical model arise also for gravitational wormholes in an

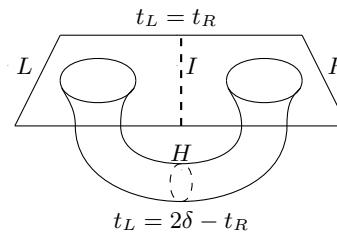


FIG. 2. Schematic representation of a wormhole corresponding to the colored lines in figure 1. The times  $t_L$  and  $t_R$  of the left and right regions are identified at the interface  $I$ . In the bulk a different identification is used that accounts for the sign flip of the time-like Killing vector at the horizon  $H$ .

exactly analogous way. As an example, we consider an eternal black hole in AdS spacetime depicted in figure 1. The dual boundary CFTs are in the TFD state [8], which can be derived from the Hartle-Hawking wave functional for the bulk geometry [14, 15] (for a review, see [16]).

We find, in exact analogy to the quantum mechanical example, a Berry phase by considering different unitary transformations given by Hamiltonian evolution of the boundary states.

As discussed in the introduction, the class of wormholes shown in figure 1 is dual to the class of states

$$|\text{TFD}_\alpha\rangle = \sum_n e^{i\alpha_n} e^{-\beta \frac{E_n}{2}} |n\rangle_L |n\rangle_R^*, \quad (10)$$

where  $\beta$  is the inverse temperature and  $E_n = (E_n^{(L)} + E_n^{(R)})/2$  are the sums of the energy eigenvalues corresponding to the left and right energy eigenstates  $|n\rangle_{L/R}^*$ . When all phases vanish, i.e.,  $\alpha_n = 0$ , (10) reduces to the standard TFD state. These additional phase factors can be incorporated in the Hartle-Hawking derivation when relating the left and the right boundary states  $|n\rangle_L$  and  $|n\rangle_R$  by an anti-unitary operator  $\Theta$  [14]. The map  $|n\rangle_L = \Theta |n\rangle_R$  is not unique. The fact that it is defined up to a phase gives rise to the phases in (10). These phases do not change the entanglement properties of the resulting state. When calculating the reduced density matrix of either CFT using (10), the phases  $\alpha_n$  drop out. As a consequence, the entanglement entropy of each of the subsystems remains insensitive to this phase. We refer the reader to the appendix for details of this calculation. The same conclusion can also be reached by computing the mixed two-point correlators  $\langle \text{TFD}_\alpha | \mathcal{O}_L \mathcal{O}_R | \text{TFD}_\alpha \rangle$  involving operators of the right and left CFTs in the time-shifted TFD state (10). These correlators turn out to be insensitive to the phases  $\alpha_n$  [17], implying unaltered entanglement properties.

We now discuss how the Berry phase arises in the gravity picture. Each field theory boundary shown in Fig. 1 has a time coordinate  $t_L$  and  $t_R$ , respectively. As shown in Fig. 2, at the interface  $I$  we have to specify an identification between the boundary times, which for convenience we choose as  $t_L = t_R$ . However, since there is no

globally defined time for the dual geometry due to the presence of the black hole horizon  $H$ , this asymptotic identification cannot hold throughout the entire bulk. In particular, since the timelike Killing vector flips sign across the horizon, a time shift  $\delta$  at the horizon needs to be taken into account, via the relation  $t_L = 2\delta - t_R$  (see Ref. [10] for further details). Together with  $t_L = t_R$ , this relation implies  $\delta = t_L = t_R$  at the boundaries. Thus, time evolution on both boundaries can be expressed using the emerging parameter  $\delta$ . As shown in [10], the additional phases appearing in the time-shifted TFD states (10) can be understood as resulting from time evolution through an identification  $\alpha_n = -2E_n\delta$ . In terms of this parameter  $\delta$ , in analogy with the quantum mechanics example we define a Berry connection for (10) as

$$A_\delta = i \langle \text{TFD}_\alpha | \partial_\delta | \text{TFD}_\alpha \rangle = -2 \sum_n E_n. \quad (11)$$

This definition follows from considering unitary transformations in the asymptotic symmetry group, which is the subgroup of bulk diffeomorphisms leaving the boundary conditions invariant. The gauge parameter of this group is  $\delta$ . For more details on the asymptotic symmetry group, we refer the reader to the appendix.

In order to show the analogy between the coupled two-spin system considered above and the gravitational example, we consider two contrasting scenarios i)  $\lambda = 0$  and ii)  $\lambda = 1$  discussed in the context of quantum mechanics, with  $\lambda$  defined below (3).

i) In the analysis of the quantum mechanical example leading to (5),  $\lambda = 0$ , which corresponds to setting  $U_2 = \mathbb{1}$ , leads to a non-trivial Berry connection. An analogous situation arises for the TFD state for the unitary operation

$$u_0(\delta) = e^{-i(H_L + H_R)\delta} \quad (12)$$

belonging to the asymptotic symmetry group. The transformation (12) can be turned into a one-sided transformation by combining with a trivial transformation as

$$\tilde{u}_0(\delta) = u_1(\delta) \cdot u_0(\delta) = e^{-2iH_L\delta}, \quad (13)$$

$$u_1(\delta) = e^{-i(H_L - H_R)\delta} \quad (14)$$

where  $u_1(\delta)$  is a trivial transformation for  $H_L = H_R$ . In order to compute the Berry connection for this unitary transformation, we note that the time-shifted TFD states (10) are obtained from the TFD states without additional phases, i.e.  $\alpha_n = 0$ , by applying (13),

$$|\text{TFD}_\alpha\rangle = \tilde{u}_0(\delta) |\text{TFD}_{\alpha=0}\rangle. \quad (15)$$

With respect to the parameter  $\delta$ , the Berry connection is then given by (11). This is the exact analogue of the quantum mechanical case with  $\lambda = 0$ . Both for the two-spin system and for the wormhole geometry, for one-sided transformations we obtain non-trivial Berry connections.

ii) According to (5), the  $\lambda = 1$  case in the quantum mechanics example corresponds to a vanishing Berry connection. An analogous situation arises for the TFD state when we consider the unitary operation (14). Since the times  $t_L$  and  $t_R$  run in opposite direction [18] as shown in Fig. 1, the transformation (14) corresponds to applying the same unitary transformation to the two subsystems as in the two-spin system. Moreover, computing the Berry connection for this transformation yields

$$A_\delta = i \langle \text{TFD}_{\alpha=0} | u_1^\dagger \partial_\delta u_1 | \text{TFD}_{\alpha=0} \rangle = 0, \quad (16)$$

in analogy to the  $\lambda = 1$  case in (5).

*Non-exact symplectic form within gravity* — These structures may be realized explicitly for a wormhole in Jackiw-Teitelboim (JT) gravity [19], consisting of AdS<sub>2</sub> gravity coupled to a dilaton scalar field. The Hamiltonians  $H_L$  and  $H_R$  are given in terms of the ratio of the dilaton values at the horizon and the AdS boundary,  $\phi_h$  and  $\phi_b$ , as  $H_L = H_R = \phi_h^2/\phi_b$  [20]. For this simple scenario, the asymptotic symmetries are given only by time translations with associated gauge parameter  $\delta$ . Clearly, the difference  $H_L - H_R$  is a trivial operator and only  $H = H_L + H_R$  generates time evolution. The associated phase space consists of variables  $\delta$  and  $\phi_h$  with symplectic form [20]

$$\omega = \frac{4\phi_h}{\phi_b} d\delta \wedge d\phi_h = d\delta \wedge dH. \quad (17)$$

As in the quantum mechanical example, this symplectic form corresponds to the Berry curvature giving rise to a Berry phase proportional to  $\alpha = 2\phi_h^2/\phi_b$ . To discuss the exactness of (17), we note that the Berry phase can be understood as the holonomy of a bundle [21]. A non-trivial holonomy arises when the considered manifold cannot be described by just one coordinate patch. Each of these patches has its own connection. Therefore, one cannot define a symplectic form as an exterior derivative of a single connection. Hence, the symplectic form cannot be globally exact. However, the connections on individual patches are related to each other by U(1) gauge transformations and yields a non-zero Berry phase. Since we find a non-vanishing Berry phase for  $\delta \neq 0$ , following the above argument, the symplectic form in (17) cannot be globally exact. This is analogous to the quantum mechanical two-spin example analyzed above using  $\mathbf{CP}^3$ , where a non-exact symplectic form (6) is also found. In the TFD example, the emergence of this Berry phase  $\alpha_n = -2E_n\delta$  can also be argued in terms of the holonomy associated to the modular Hamiltonian [22–24].

*Discussion and conclusion* — The non-exactness of the symplectic structure and the corresponding Berry phases associated to a gravitational wormhole are equivalently found in analyzing the quantum mechanical two-spin system. This further exemplifies the surprising similarity between quantum mechanical models and gravitational



wormholes. In the gravitational setup, wormholes arise naturally from the non-local structure of the spacetime due to the presence of the black hole horizon. In quantum mechanical systems, where locality is manifest, this feature is realised by intricate group theoretical structures. To make this apparent, using group theoretic arguments, we have actually identified the entangled degrees of freedom in our quantum mechanical system which are responsible for creating a wormhole geometry in spin space. This may be viewed as a manifestation of *entanglement creating spacetime* which lies at the heart of understanding AdS/CFT duality [3, 25–27].

In particular, we found that both for wormholes and in simple qubit systems, there are entangled states that have different Berry phases while sharing the same entanglement entropy. For quantum mechanics, this analysis might be probed on a number of experimental platforms. Generally measurements of both quantum entanglement and of Berry phases involve interference between the original starting state and a rotated one for an ensemble of identical quantum states. Apart from the two-spin systems that we discussed above, which are toy models for the multiple spin-qubits accessible in liquid-state nuclear magnetic resonance [28], also quantum dots coupled to an optical cavity [29] and superconducting quantum circuits offer experimental platforms for quantum tomography on controlled qubit pairs [30–32]. A further avenue to connect to experiment arises from the fact that TFD states can be experimentally prepared to a high accuracy using quantum approximate optimization algorithm for transverse field Ising models [33]. Modifying this algorithm to realize time-shifted TFD states as in (10) will provide an experimental realization of the proposed entanglement structure in the context of TFD states.

*Acknowledgments* — We thank Emma Loos and Anna-Lena Weigel for useful discussions. S.B., M.D., R.M., J.v.d.B. and J.E. acknowledge support by the Deutsche Forschungsgemeinschaft (DFG, German Research Foundation) under Germany’s Excellence Strategy through the Würzburg-Dresden Cluster of Excellence on Complexity and Topology in Quantum Matter - ct.qmat (EXC 2147, project-id 390858490). The work of S.B., M.D., R.M. and J.E. is furthermore supported via project-id 258499086 - SFB 1170 ‘ToCoTronics’. The work of S.B. is supported by the Alexander von Humboldt postdoctoral fellowship.

## APPENDIX

*Entanglement entropy for the two-spin model* — Since this is part of our main statement, we show explicitly that all rotated states discussed in the quantum mechanical example in the main text have the same entanglement entropy, as stated in (4).

We start by applying the rotation  $U(\lambda) = U_1 \otimes U_2(\lambda)$  defined below (3) on the state  $|\psi_0\rangle$  given in (2). This yields a state of the form

$$|\tilde{\psi}_0\rangle = a_1 |\uparrow\uparrow\rangle + a_2 |\uparrow\downarrow\rangle + a_3 |\downarrow\uparrow\rangle + a_4 |\downarrow\downarrow\rangle, \quad (\text{A.1})$$

with coefficients  $a_i$  depending on  $\theta$ ,  $\varphi$  and  $\lambda$ . The explicit expressions for  $a_i$  are lengthy and are not given here. We compute the entanglement entropy first for  $|\tilde{\psi}_0\rangle$  and subsequently, to show that the entanglement has not changed, for the state  $|\psi_0\rangle$  without the rotation  $U$ . Starting with  $|\tilde{\psi}_0\rangle$  and the second spin to be traced out, the resulting reduced density matrix is

$$\begin{aligned} \tilde{\rho}_1 = & \left( |a_1|^2 + |a_2|^2 \right) |\uparrow\rangle \langle\uparrow| + \left( |a_3|^2 + |a_4|^2 \right) |\downarrow\rangle \langle\downarrow| \\ & + (a_1 a_3^* + a_2 a_4^*) |\uparrow\rangle \langle\downarrow| + (a_1^* a_3 + a_2^* a_4) |\downarrow\rangle \langle\uparrow|. \end{aligned} \quad (\text{A.2})$$

Inserting the coefficients  $a_i$  explicitly, we find that  $\tilde{\rho}_1$  does not depend on the parameter  $\lambda$ . This is expected since the transformation  $U_2$  acts on the second spin. Since the density matrix does not depend on  $\lambda$ , also the entanglement entropy can not depend on it and is therefore the same for all of the different rotations.

On the other hand, tracing over the first spin, the density matrix becomes

$$\begin{aligned} \tilde{\rho}_2 = & \left( |a_1|^2 + |a_3|^2 \right) |\uparrow\rangle \langle\uparrow| + \left( |a_2|^2 + |a_4|^2 \right) |\downarrow\rangle \langle\downarrow| \\ & + (a_1 a_2^* + a_3 a_4^*) |\uparrow\rangle \langle\downarrow| + (a_1^* a_2 + a_3^* a_4) |\downarrow\rangle \langle\uparrow|. \end{aligned} \quad (\text{A.3})$$

Inserting the explicit expressions for  $a_i$  in terms of  $\varphi$ ,  $\theta$  and  $\lambda$ , we find that the density matrix still depends on  $\lambda$ . However, calculating the entanglement entropy for  $\tilde{\rho}_2$ , the dependence on  $\lambda$  drops out and we find the same result as for  $\tilde{\rho}_1$ . This is expected since the entanglement entropy calculated for  $\tilde{\rho}_1$  does not depend on  $\theta$  or  $\varphi$ ; a rescaling of these variables therefore must not play a role for the entanglement entropy.

Now we calculate the entanglement entropy for the unrotated state  $|\psi_0\rangle$ . The reduced density matrix for tracing out the second spin is

$$\rho_1 = \frac{1 - \sin \alpha}{2} |\uparrow\rangle \langle\uparrow| + \frac{1 + \sin \alpha}{2} |\downarrow\rangle \langle\downarrow|, \quad (\text{A.4})$$

where  $\tan \alpha = 2\mu_B B/J$ . Tracing out the first spin yields the same result (A.4) with the two coefficients exchanged.

The resulting entanglement entropy is the same as we found for the state  $|\tilde{\psi}_0\rangle$ , given explicitly by the expression

$$S_{\text{EE}} = \ln\left(\frac{2}{\cos\alpha}\right) + \sin\alpha \ln\left(\frac{1 - \sin\alpha}{\cos\alpha}\right). \quad (\text{A.5})$$

So we find that the entanglement between the spins is not affected by the unitary rotations, independently of which system we trace out. In the limit  $B \rightarrow 0$  (that is  $\alpha \rightarrow 0$ ) we recover the well known result  $S_{\text{EE}} = \ln 2$ .

Now we show in general that the entanglement entropy is not affected by a two-sided factorized unitary transformation. Consider a generic state  $|\chi\rangle$  related to a different state  $|\phi\rangle$  by a unitary transformation  $U$  that can be written as  $U = U_1 \otimes U_2$ . Further consider  $|\phi\rangle$  to be a general pure state in a bipartite system  $|\phi\rangle = c_{ij} |i\rangle_1 |j\rangle_2$ , where  $c_{ij}$  are arbitrary coefficients (up to the normalisation condition). We compute the reduced density matrix, tracing out the second system,

$$\begin{aligned} \rho_1^\chi &= \text{tr}_2(|\chi\rangle\langle\chi|) = \text{tr}_2(U|\phi\rangle\langle\phi|U^\dagger) \\ &= c_{ij}c_{lk}^* \text{tr}_2\left(U_1|i\rangle_1 U_2|j\rangle_2 \langle l|_1 U_1^\dagger \langle k|_2 U_2^\dagger\right) \\ &= c_{ij}c_{lk}^* \langle n|_2 \left(U_1|i\rangle_1 U_2|j\rangle_2 \langle l|_1 U_1^\dagger \langle k|_2 U_2^\dagger\right) |n\rangle_2 \\ &= c_{ij}c_{lk}^* U_1|i\rangle_1 \langle l|_1 U_1^\dagger \langle n| U_2|j\rangle_2 \langle k| U_2^\dagger |n\rangle \\ &= c_{ij}c_{lk}^* U_1|i\rangle_1 \langle l|_1 U_1^\dagger \langle k| U_2^\dagger U_2|j\rangle \\ &= c_{ij}c_{lj}^* U_1|i\rangle_1 \langle l|_1 U_1^\dagger = U_1 \rho_1^\phi U_1^\dagger. \end{aligned} \quad (\text{A.6})$$

The transformation on the system which is traced over drops out. The reduced density matrix is only affected by the transformation on the system which remains present. However the specific observable of entanglement entropy is not affected by this transformation, since the calculation of the entanglement entropy reduces to an eigenvalue problem for  $\rho_1$ . For the eigenvalue problem it is not important whether we calculate with  $\rho_1^\chi$  or  $\rho_1^\phi$ . Therefore the states  $|\chi\rangle$  and  $|\phi\rangle$  have the same amount of entanglement, independently of the unitary transformation that relates them.

*Bundle connection in the  $\mathbf{CP}^3$  analysis* — Here we explain in more detail the calculation of the connection in the  $\mathbf{CP}^3$  analysis below (9).

The transformation  $U_1$  acting on the first spin is given in (3).  $U_2$  is then given by  $U_2(\varphi, \theta) = U_1(\lambda\varphi, \lambda\theta)$ . The  $U(1)$  factor in the decomposition of  $SU(4)$  leads to a negative sign for the second  $SU(2)$  compared to the first one [13]. To account for this relative sign in the transformation  $U_2$  acting on the second spin, we have to replace  $\sigma_i \rightarrow -\sigma_i$  in  $U_2$ ,

$$U_2 \xrightarrow{\sigma_i \rightarrow -\sigma_i} \tilde{U}_2 = e^{i\lambda\frac{\varphi}{2}\sigma_z} e^{i\lambda\frac{\theta}{2}\sigma_y} e^{-i\lambda\frac{\varphi}{2}\sigma_z} = U_2^T. \quad (\text{A.7})$$

We observe here that the same expression for  $\tilde{U}_2$  can be obtained from  $U_2$  by reversing the sign of  $\lambda$ . Using

$\tilde{g} = U_1 \otimes \tilde{U}_2$  in (8) with (9), we obtain, with a proper normalization factor,

$$A = \frac{\sin\alpha}{2} \{(1 - \cos\theta) - \lambda(1 - \cos(\lambda\theta))\} d\varphi. \quad (\text{A.8})$$

This is the same expression as in (5) which vanishes for  $\lambda = 1$ .

*Time-shifted TFD states from a path integral* — Here we briefly review how the generalised TFD state as in (10) is computed from a path integral. We discuss in more detail how the additional phase factors  $\alpha_n$  which lead to the Berry phase can be naturally incorporated in this derivation.

We first sketch how the TFD state without additional phase factors (i.e. (10) with  $\alpha_n = 0 \forall n$ ) arises as the groundstate  $|\Omega\rangle$  at infinite past from a path integral [16]. This calculation leads to the Hartle-Hawking wave function  $\Psi_{\text{HH}} = \langle\phi|\Omega\rangle$ . Up to a normalisation factor, this wave function is defined by a Euclidean path integral

$$\Psi_{\text{HH}} \propto \int \mathcal{D}g \mathcal{D}\phi \exp(-S_E[g, \phi]), \quad (\text{A.9})$$

where  $\phi$  is some matter field (for instance, a real scalar) and  $g$  specifies the geometry on which  $\phi$  propagates. The calculation of the path integral relies on saddle point approximations for the metric. In our case, we specify  $g$  to the eternal Schwarzschild AdS metric. We then consider a real scalar field on that geometry. For some generic state  $|\kappa\rangle$ , the groundstate is calculated as

$$\langle\phi|\Omega\rangle = \frac{1}{\langle\Omega|\kappa\rangle} \lim_{t_E \rightarrow \infty} \langle\phi| e^{-t_E H} |\kappa\rangle. \quad (\text{A.10})$$

Up to a normalisation factor this corresponds to

$$\langle\phi|\Omega\rangle \propto \int_{\hat{\phi}(t_E=-\infty)=0}^{\hat{\phi}(t_E=0)=\phi} \mathcal{D}\hat{\phi} \exp(-S_E[\hat{\phi}]). \quad (\text{A.11})$$

$S_E$  is the Euclidean action for the scalar field on the geometry  $g$  and  $H$  is the corresponding Hamiltonian. Instead of integrating the lower half of the Euclidean plane by time evolution using the Hamiltonian, it is convenient to make use of the Rindler decomposition. In Rindler coordinates, the Hamiltonian is replaced by the boost operator  $K_x$  (we choose a boost in  $x$ -direction for simplicity) and the integration is along the angular direction  $\varphi$ . Integrating over the half plane is then easily seen to be a rotation by  $\pi$ . Solving the path integral (A.11) requires a careful consideration of the boundary conditions: in the path integral we introduced  $\phi$  as the boundary condition at  $t_E = 0$ . However using the boost operator we find that the ‘initial’ state is on the same time slice as the ‘final’ state. We can fix this by splitting  $\phi$  across the origin as  $\phi(x < 0) = \phi_L$  and  $\phi(x > 0) = \phi_R$ , that is  $\phi_R$  is the initial and  $\phi_L$  is the final state. This is described by an anti-unitary operator  $\Theta$  containing the time reversal

operator defined in QFT. Initial ( $|\phi_R\rangle$ ) and final ( $|\phi_R\rangle$ ) state are related by  $\langle\phi_R| = \Theta|\phi_R\rangle$ . This implies that  $K_x$  may act only on the left states. The solution to the path integral (A.11) is then written as

$$\langle\phi|\Omega\rangle = \langle\phi_L\phi_R|\Omega\rangle = \langle\phi_L|e^{-\pi K_L}\Theta|\phi_R\rangle. \quad (\text{A.12})$$

Inserting a complete set of eigenstates to  $K_L$  and using the anti-linearity of  $\Theta$  we find

$$\begin{aligned} \langle\phi|\Omega\rangle &= \sum_n \langle\phi_L|e^{-\pi K_L}|n_L\rangle\langle n_L|\Theta|\phi_R\rangle \\ &= \sum_n e^{-\pi E_n} \langle\phi_L|n_L\rangle\langle\phi_R|\Theta^\dagger|n_L\rangle \end{aligned} \quad (\text{A.13})$$

To write  $|\Omega\rangle$  manifestly as a sum over left and right states one has to impose the relation  $|n_R\rangle^* \propto \Theta^\dagger|n_L\rangle$ . As already indicated, there is a freedom in choosing this relation: while an equality leads to the commonly known expression for the TFD state, we can also choose to include a phase factor  $e^{-i\alpha_n}$ . As we will show in the next section, this choice is possible since it does not change the entanglement structure between the left and right subsystems. Applying this to (A.13), i.e. the TFD state, we find

$$|\text{TFD}_\alpha\rangle = \sum_n e^{i\alpha_n} e^{-\pi\omega_n} |n_L\rangle |n_R\rangle^*. \quad (\text{A.14})$$

This is the non-normalized TFD state with additional phases.

Note that the explicit calculation above was done for a Rindler observer with unit acceleration, corresponding to a temperature  $\beta = 2\pi$ . Therefore we can rewrite the result to

$$|\text{TFD}_\alpha\rangle = \sum_n e^{i\alpha_n} e^{-\beta\frac{E_n}{2}} |n_L\rangle |n_R\rangle^* \quad (\text{A.15})$$

as in (10) in the main text.

*Entanglement entropy for time shifted TFD states* — Here we show that the additional phases in the time-shifted TFD state (10) do not change the entanglement entropy by explicit calculation of the reduced density matrix of the left subsystem  $\rho_L$  (the calculation of  $\rho_R$  works analogously):

$$\begin{aligned} \rho_L &= \text{tr}_R(|\text{TFD}_\alpha\rangle\langle\text{TFD}_\alpha|) \\ &= \sum_{m,n} e^{-\frac{\beta}{2}(E_n+E_m)} e^{i(\alpha_n-\alpha_m)} \text{tr}_R(|n\rangle_L|n\rangle_R\langle m|_L\langle m|_R) \\ &= \sum_{m,n,k} e^{-\frac{\beta}{2}(E_n+E_m)} e^{i(\alpha_n-\alpha_m)} |n\rangle_L\langle m|_L\langle k|_R\langle m|k\rangle_R \\ &= \sum_{m,k} e^{-\frac{\beta}{2}(E_k+E_m)} e^{i(\alpha_k-\alpha_m)} |k\rangle_L\langle m|_L\langle m|k\rangle_R \\ &= \sum_k e^{-\beta E_k} |k\rangle_L\langle k|_L. \end{aligned} \quad (\text{A.16})$$

The reduced density matrix is independent of the phase factors. It is the same as the non-normalized thermal density matrix obtained from the TFD state without additional phases  $\alpha_n = 0 \forall n$ . Since the phases drop out, the entanglement entropy will be unchanged.

*Asymptotic symmetries in AdS spacetime* — Here we give more details about asymptotic symmetries in AdS spacetimes, mentioned below (11).

Since AdS is a spacetime with boundary, for a well defined variational principle it is necessary to impose boundary conditions on the dynamical fields. The variation of an action on a manifold  $\mathcal{M}$  with  $\text{AdS}_{d+1}$  background has boundary terms

$$\delta S \supset \int_{\partial\mathcal{M}} d^d x \sqrt{\gamma} T_{ij} \delta\gamma^{ij} \quad (\text{A.17})$$

where  $\gamma$  is the metric induced on the boundary.  $T_{ij}$  can be defined as the boundary energy momentum tensor.  $\delta\gamma^{ij}$  can be fixed such that the variation of the action vanishes, that is imposing Dirichlet boundary conditions

$$\gamma^{ij} = \mathcal{C}^{ij}, \quad (\text{A.18})$$

where  $\mathcal{C}^{ij}$  is a tensor with constant entries.

These boundary conditions are not preserved by any arbitrary diffeomorphism. The subset of diffeomorphisms which do preserve (A.18) are called asymptotic symmetries. These change (A.18) only by additional constants  $c^{ij}$  for each component of  $\mathcal{C}^{ij}$ , that is the variation of  $\gamma^{ij}$  still vanishes.

Asymptotic symmetries are generated by Killing vectors  $\xi$  that are also an isometry of the boundary metric. This implies

$$\gamma_\mu^\alpha \gamma_\nu^\beta \nabla_{(\alpha} \xi_{\beta)} = 0. \quad (\text{A.19})$$

There is however another important distinction of asymptotic symmetries depending on the values of  $c^{ij}$ : there are diffeomorphisms where  $c^{ij} = 0$ , called trivial in the following, and also such where  $c^{ij} \neq 0$ . The latter ones will lead to a change in the boundary phase space, proportional to these constants.

Since the boundary includes the time dimension, time translations will always be a part of the asymptotic symmetries. An explicit example for a time translation with  $c^{ij} \neq 0$  is given by

$$\xi_0 = e^{-i(H_L+H_R)\delta}. \quad (\text{A.20})$$

The constants  $c^{ij}$  arise as the additional phases in (10). In the JT gravity example, the asymptotic symmetries are only time translations and  $c^{ij}$  has only one component. Noting that  $\delta$  is not a coordinate one can check that the diffeomorphism  $\xi_0$  given in (A.20) satisfies (A.19) and describes such time translations. Acting with an asymptotic symmetry on the TFD state, the constant will appear as the additional phase containing the emerging time parameter  $\delta$  as  $c = \alpha_n = -2E_n\delta$  as in (10). If

$\delta = 0$ , the TFD state does not receive any additional phase and the associated diffeomorphism is trivial.

- 
- [1] S. Ryu and T. Takayanagi, “Holographic derivation of entanglement entropy from AdS/CFT,” *Phys. Rev. Lett.* **96**, 181602 (2006), [arXiv:hep-th/0603001](#).
- [2] J. M. Maldacena, “The Large N limit of superconformal field theories and supergravity,” *Adv. Theor. Math. Phys.* **2**, 231–252 (1998), [arXiv:hep-th/9711200](#).
- [3] J. M. Maldacena and L. Susskind, “Cool horizons for entangled black holes,” *Fortsch. Phys.* **61**, 781–811 (2013), [arXiv:1306.0533 \[hep-th\]](#).
- [4] J. Wheeler, “Geons,” *Phys. Rev.* **97**, 511–536 (1955).
- [5] D. Garfinkle and A. Strominger, “Semiclassical wheeler wormhole production,” *Physics Letters B* **256**, 146–149 (1991).
- [6] S. Novikov, “The hamiltonian formalism and a many-valued analogue of morse theory,” *Uspekhi Matematicheskikh Nauk* **37**, 3–49 (1982).
- [7] H. Verlinde, “Wormholes in Quantum Mechanics,” (2021), [arXiv:2105.02129 \[hep-th\]](#).
- [8] J. M. Maldacena, “Eternal black holes in anti-de Sitter,” *JHEP* **04**, 021 (2003), [arXiv:hep-th/0106112](#).
- [9] K. Papadodimas and S. Raju, “Local Operators in the Eternal Black Hole,” *Phys. Rev. Lett.* **115**, 211601 (2015), [arXiv:1502.06692 \[hep-th\]](#).
- [10] H. Verlinde, “ER = EPR revisited: On the Entropy of an Einstein-Rosen Bridge,” (2020), [arXiv:2003.13117 \[hep-th\]](#).
- [11] Rainer Blatt and David Wineland, “Entangled states of trapped atomic ions,” *Nature* **453**, 1008–1015 (2008).
- [12] M. Nakahara, *Geometry, topology and physics* (2003).
- [13] H. Georgi, *Lie Algebras In Particle Physics: from Isospin To Unified Theories*, Vol. 54 (Westview Press, 1999).
- [14] J. B. Hartle and S. W. Hawking, “Path Integral Derivation of Black Hole Radiance,” *Phys. Rev. D* **13**, 2188–2203 (1976).
- [15] W. Israel, “Thermo field dynamics of black holes,” *Phys. Lett. A* **57**, 107–110 (1976).
- [16] D. Harlow, “Jerusalem Lectures on Black Holes and Quantum Information,” *Rev. Mod. Phys.* **88**, 015002 (2016), [arXiv:1409.1231 \[hep-th\]](#).
- [17] K. Papadodimas and S. Raju, “Remarks on the necessity and implications of state-dependence in the black hole interior,” *Phys. Rev. D* **93**, 084049 (2016), [arXiv:1503.08825 \[hep-th\]](#).
- [18] This follows from the fact that the bulk Killing vector switches sign at the horizon. This is accounted for by relating the CFT times at the left and right boundaries to the Schwarzschild times in the respective bulk wedges with a relative flip of sign. Note that this is independent of any additional phases in the TFD state (10).
- [19] G. Sárosi, “AdS<sub>2</sub> holography and the SYK model,” *PoS Modave2017*, 001 (2018), [arXiv:1711.08482 \[hep-th\]](#).
- [20] D. Harlow and D. Jafferis, “The Factorization Problem in Jackiw-Teitelboim Gravity,” *JHEP* **02**, 177 (2020), [arXiv:1804.01081 \[hep-th\]](#).
- [21] B. Simon, “Holonomy, the quantum adiabatic theorem, and berry’s phase,” *Phys. Rev. Lett.* **51**, 2167–2170 (1983).
- [22] B. Czech, L. Lamprou, S. Mccandlish, and J. Sully, “Modular Berry Connection for Entangled Subregions in AdS/CFT,” *Phys. Rev. Lett.* **120**, 091601 (2018), [arXiv:1712.07123 \[hep-th\]](#).
- [23] B. Czech, L. Lamprou, and L. Susskind, “Entanglement Holonomies,” (2018), [arXiv:1807.04276 \[hep-th\]](#).
- [24] B. Czech, J. De Boer, D. Ge, and L. Lamprou, “A modular sewing kit for entanglement wedges,” *JHEP* **11**, 094 (2019), [arXiv:1903.04493 \[hep-th\]](#).
- [25] M. Van Raamsdonk, “Comments on quantum gravity and entanglement,” (2009), [arXiv:0907.2939 \[hep-th\]](#).
- [26] M. Van Raamsdonk, “Building up spacetime with quantum entanglement,” *Gen. Rel. Grav.* **42**, 2323–2329 (2010), [arXiv:1005.3035 \[hep-th\]](#).
- [27] B. Czech, J. Karczmarek, F. Nogueira, and M. Van Raamsdonk, “The Gravity Dual of a Density Matrix,” *Class. Quant. Grav.* **29**, 155009 (2012), [arXiv:1204.1330 \[hep-th\]](#).
- [28] C. A. Ryan, M. Laforest, and R. Laflamme, “Randomized benchmarking of single- and multi-qubit control in liquid-state NMR quantum information processing,” *New Journal of Physics* **11**, 013034 (2009), [arXiv:0808.3973 \[quant-ph\]](#).
- [29] A. Imamoglu, D. D. Awschalom, G. Burkard, D. P. DiVincenzo, D. Loss, M. Sherwin, and A. Small, “Quantum information processing using quantum dot spins and cavity qed,” *Phys. Rev. Lett.* **83**, 4204–4207 (1999), [arXiv:quant-ph/9904096](#).
- [30] M. Steffen, M. Ansmann, R. C. Bialczak, N. Katz, E. Lucero, R. McDermott, M. Neeley, E. M. Weig, A. N. Cleland, and J. M. Martinis, “Measurement of the entanglement of two superconducting qubits via state tomography,” *Science* **313** (2006).
- [31] M. H. Devoret and R. J. Schoelkopf, “Superconducting Circuits for Quantum Information: An Outlook,” *Science* **339**, 1169–1174 (2013).
- [32] C. Song, K. Xu, W. Liu, C.-P. Yang, S.-B. Zheng, H. Deng, Q. Xie, K. Huang, Q. Guo, L. Zhang, P. Zhang, D. Xu, D. Zheng, X. Zhu, H. Wang, Y.-A. Chen, C.-Y. Lu, S. Han, and J.-W. Pan, “10-qubit entanglement and parallel logic operations with a superconducting circuit,” *Phys. Rev. Lett.* **119**, 180511 (2017), [arXiv:1703.10302 \[quant-ph\]](#).
- [33] D. Zhu, S. Johri, N. M. Linke, K. A. Landsman, N. H. Nguyen, C. H. Alderete, A. Y. Matsuura, T. H. Hsieh, and C. Monroe, “Generation of thermofield double states and critical ground states with a quantum computer,” *Proc. Nat. Acad. Sci.* **117**, 25402–25406 (2020), [arXiv:1906.02699 \[quant-ph\]](#).